ACS POLYMERS Au
AN OPEN ACCESS JOURNAL OF THE AMERICAN CHEMICAL SOCIETY

pubs.acs.org/polymerau

Article

Programmed Macromolecular Assembly by Dipole−Dipole Interactions with Aggregation-Induced Enhanced Emission in Aqueous Medium

Aritra Rajak and Anindita Das*

Cite This: *ACS Polym. Au* 2022, 2, 223−231

Read Online

ACCESS | Metrics & More | Article Recommendations | Supporting Information

ABSTRACT: Self-assembling polymers by bioinspired directional supramolecular interactions currently hold great scientific and technological interests. Herein, we report an unorthodox strategy based on a dipole−dipole interaction-mediated extended antiparallel dipolar assembly of a model merocyanine (MC) dye for maneuvering the self-assembly of a highly water-soluble MC-functionalized block copolymer (**P2**). Unlike traditional amphiphilic block copolymers featuring distinct hydrophobic segments (flexible aliphatic hydrocarbon chains or rigid nonpolar aromatic scaffolds), **P2** comprises polyethylene glycol monomethyl ether (PEG) as a hydrophilic block and an unconventional structure-directing acrylate block functionalized with polar MC-dyes in the side chains of every repeat unit. In the absence of any additional hydrophobic assistance, **P2** spontaneously self-assembles in water through the continuous opposite alignment of its pendant MCs by multiple dipole−dipole interactions to cancel out their ground state dipole moments, which initially generates an H-aggregated species with ill-defined morphology (**Aggregate 1**). Upon thermal annealing, **Aggregate 1** reorganizes into higher-order core−shell nanodisc-like structures (**Aggregate 2**) driven by the orthogonal π-stacking interactions of the rigid aromatic framework derived from the extended cofacial MC-stacks. The aromatic interiors of the nanodiscs gain colloidal stability from the externally decorated hydrophilic PEG chains. While the initially formed **Aggregate 1**, predominantly by dipole−dipole interactions, showed remarkable thermal stability due to the cooperative effect of the polymer chain, the hierarchical assembly guided by relatively weaker dispersion forces of the MC-stacked π-surfaces could be tailored by dilution or thermal treatment. Such organized packing of pendant MCs by the dual effect of dipole−dipole interactions and π-stacking conferred several exciting properties to the **P2** assembly in water. Long-range ordered antiparallel stacking of the pendant MCs rendered outstanding aggregation-induced enhanced emission (AIEE) properties to the resultant nanostructures in water with increased fluorescence lifetime, quantum yield, and Stokes shift compared to nonaggregating **P2** in $CHCl_3$. The remarkable thermal and kinetic stability of the nanodiscs, their guest loading ability, and very low critical aggregation concentration (CAC) were demonstrated by Förster resonance energy transfer (FRET) studies with an encapsulated donor−acceptor dye pair.

KEYWORDS: *Dipole−Dipole Interaction, Merocyanine, Supramolecular Assembly, Polymeric Nanostructures, Aggregation-Induced Enhanced Emission*

INTRODUCTION

Noncovalent interactions play a vital role in controlling the macroscopic architectures and complex functions of naturally occurring biomacromolecules such as proteins, nucleic acids, and many others.[1,2] Over recent years, bioinspired amphiphilic macromolecules and peptides featuring specific molecular recognizing motifs have been extensively explored with diverse synthetic scaffolds[3−6] to gain control over their folding or assembly processes, stability, dynamics, stimuli-responsiveness, etc. An in-depth understanding of how the structural parameters affect some of these properties is highly desirable for their efficient performances in most applications. Nevertheless, a majority of reports on supramolecularly engineered macromolecular assemblies are based on the utilization of hydrogen (H)-bonding interactions,[7,8] metal−ligand coordination,[9,10] aromatic charge-transfer interactions,[11] specific host−guest interactions,[12−14] and, more recently, halogen bonding.[15−18]

Self-complementary dipole−dipole interactions in dipolar push−pull type molecules are analogous to H-bonding in terms of their binding strength, directionality, tunability, and electrostatic nature of their mode of interactions.[19] Unlike H-bonding, dipolar interactions are much less reported in dictating supramolecular assemblies of diverse π-systems.[19−26]

Received: November 15, 2021
Revised: January 6, 2022
Accepted: January 6, 2022
Published: January 20, 2022

https://doi.org/10.1021/acspolymersau.1c00054
ACS Polym. Au 2022, 2, 223−231

Scheme 1. Synthetic Route to P2 from P1 by Postpolymerization Modification (Top) and Its Proposed Self-Assembly Model in Water (Bottom)

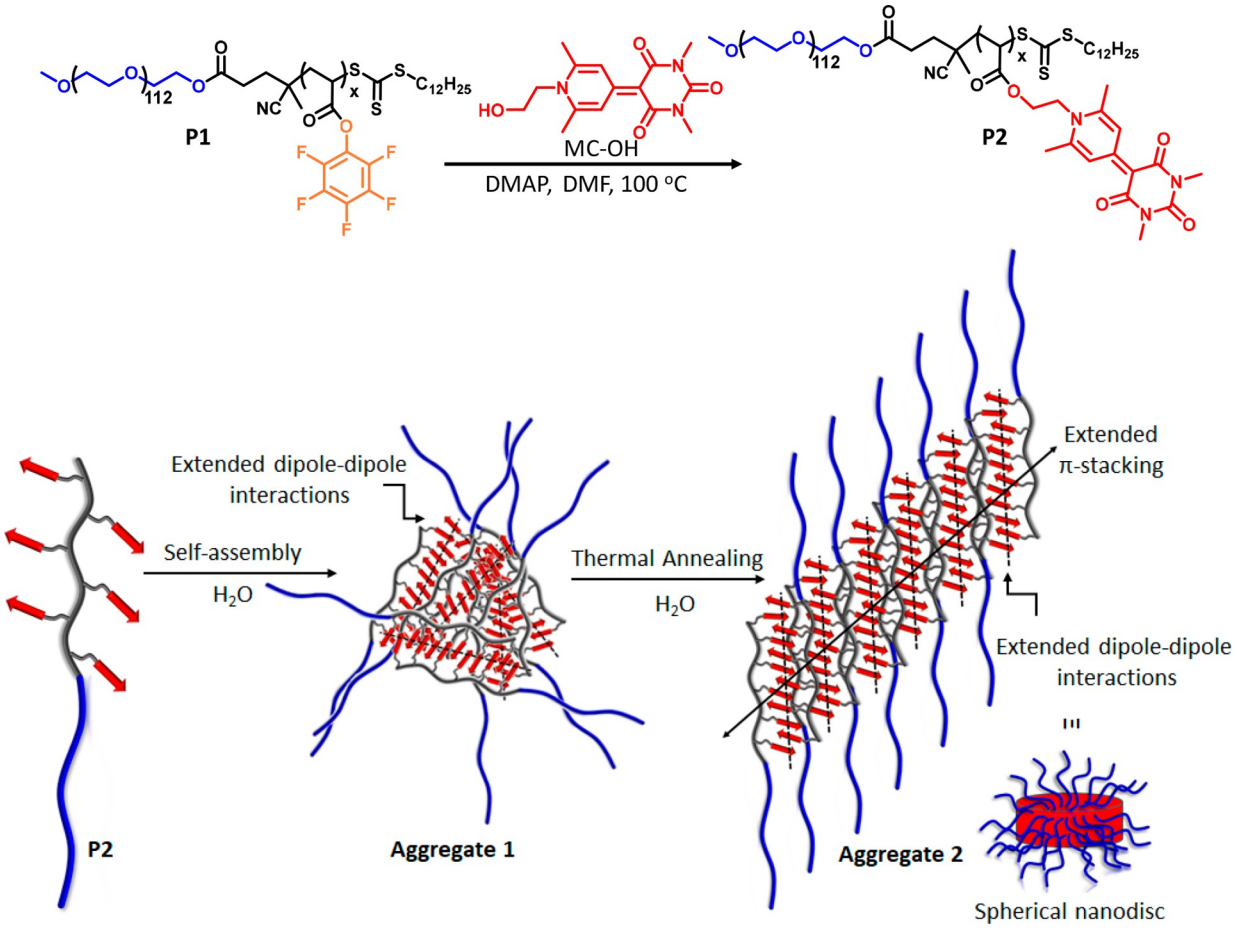

Würthner and co-workers have extensively investigated directional dipole−dipole interaction-mediated dimer aggregations in a unique class of D-π-A push−pull chromophores called merocyanines (MCs)[19] that possess a wide range of ground state dipole moments (7−18 D) depending upon the chemical structures of their heterocyclic donor (D) and acceptor (A) rings and the extent of π-conjugation between them. MCs are known to organize into discrete centrosymmetric antiparallel dimers with extremely high association constants ($\sim 10^6$ M^{-1}) in nonpolar solvents, to neutralize their ground state dipole moments.[27,28] As a result, individual merocyanines have a very low propensity to undergo extended antiparallel stacking, which is reported to be anticooperative in some cases.[29] This makes MCs distinct with respect to other commonly studied π-scaffolds that assemble via weak dispersion forces. Only a handful of examples are known on the long-range ordered antiparallel cofacial stacking of MCs in bis-merocyanine-based building blocks[30−33] or foldamers derived from short oligomers,[34,35] that too mostly limited to organic solvents. The unique combination of the high directionality and binding strength of MCs has been explored in constructing elegant supramolecular architectures in small building blocks.[19] Nevertheless, the role of dipolar interactions of MCs in engineering macromolecular assemblies is an underdeveloped area.[36,37] MC-bound polymers have been earlier studied for developing second-order nonlinear optical (NLO) materials.[38,39] Recently, spiropyran-conjugated polymers[40−42] have been studied in designing photoresponsive or mechanochromic dynamic materials due to the known ability of spiropyran to switch to its planar MC form by either photoisomerization or mechanical forces. However, the impact of dipolar interactions of MCs has been overlooked in most of these systems. To the best of our knowledge, there is no report on the utilization of the long-range ordered extended antiparallel cofacial stacking of MCs to entirely dictate the self-assembly events of highly flexible polymer chains in water. Owing to their exciting optical and conducting properties,[43] and promising response in photovoltaics,[44] it is anticipated that MCs can bestow additional functional properties to the MC-functionalized polymers, besides playing the key role of a supramolecular structure-directing entity.

We have recently reported an interesting example of cross-linked micelles derived from a block copolymer of poly(ethylene glycol)-*block*-poly(styrene) (PEG-*b*-PS) with ∼18% functionalization with a model MC-dye statistically distributed in the hydrophobic PS segment.[37] In aqueous milieu, the solvophobic collapse of the flexible PS block induced random dimerization of the statistically distributed MCs by their dipole−dipole interactions, leading to supramolecularly cross-linked polymeric micelles. It was realized that the pendant MCs were unable to dominate the polymer chain packing. Rather, the formation of discrete MC-dimers within the polymeric micelles was a consequence of the nondirectional hydrophobic effect of the PS segment in water. This conferred additional stability and photoluminescent properties to the supramolecularly cross-linked polymeric micelles but no

https://doi.org/10.1021/acspolymersau.1c00054
ACS Polym. Au 2022, 2, 223−231

structural precision.[37] This further prompted us to explore the effect of an explicitly MC-guided polymer assembly in water in the absence of any additional hydrophobic assistance, to avoid anticipated influences of other determining factors like solvophobic effect, packing parameters, and imbalance in the hydrophobic/hydrophilic block ratio. This is rather more challenging to achieve as, the MCs being dipolar, their binding strength is known to be much weaker in polar solvents[19,27] unlike conventional hydrophobic π-conjugated chromophore assemblies.[45,46]

To explore such possibilities, we have synthesized a new block copolymer **P2** by postpolymerization modification[47,48] from **P1** (Scheme 1), which is different from the earlier reported MC-functionalized PEG-*b*-PS polymer[37] as, herein, the hydrophobic PS segment was completely replaced with an MC-anchored polyacrylate block, while the hydrophilic chain was derived from PEG (Scheme 1). In this Article, we have demonstrated an unprecedented impact of the extended dipolar aggregation of MCs on the self-assembly, morphology, and photophysical properties of **P2** in water with outstanding aggregation-induced enhanced emission (AIEE) behavior.[49−51]

RESULTS AND DISCUSSION

Synthesis and Characterization

The prepolymer **P1** was synthesized by reversible addition−fragmentation chain-transfer (RAFT) polymerization of pentafluorophenyl acrylate (PFPA) monomer using a PEG-based macro-chain-transfer agent (**PEG_{5000}-CTA**) in the presence of azobis(isobutyronitrile) (AIBN) in benzene at 80 °C (Supporting Information). The chain extension was confirmed from the size exclusion chromatography (SEC), which showed a monomodal peak shifted to the lower retention time with respect to the **PEG_{5000}-CTA** (Figure S1). **P2** was obtained from **P1** by postpolymerization transesterification of the activated pentafluorophenyl ester (PFP-ester) groups with a hydroxy-functionalized MC-dye (**MC-OH**).[37] Quantitative substitution of the PFP-ester was confirmed from FTIR and ^{19}F NMR spectroscopy. This was evident from the complete disappearance of the PFP-ester carbonyl stretching at 1783 cm^{-1} in the FTIR spectrum (Figure 1a) and aromatic fluorine signals in the ^{19}F NMR spectrum of **P2** (Figure 1b). Further, the UV−vis absorption spectrum of **P2** revealed a new band corresponding to the absorbance of MC with λ_{max} = ∼381 nm in $CHCl_3$ (Figure S2) matching with the absorbance of the acetylated **MC-OH** (**MC-OAc**).[36] The ^{1}H NMR spectrum of **P2** showed new peaks at 8.97 ppm (H_a), 3.34 ppm (H_d), and 2.64 ppm (H_e) corresponding to the attached MC-dye (Figure 1c), in addition to the signals from the PEG chain. From the integrals of the MC (H_a) and methylene proton (H_f) of PEG_{5000}, the degree of polymerization (DP) of MC-block was estimated to be ∼11. The molar mass of **P2** from the ^{1}H NMR spectrum was calculated to be ∼8950 g/mol.

Self-Assembly Studies in Water

The UV−vis absorption spectrum of **P2** (c = 0.125 mg/mL) in a "good" solvent like $CHCl_3$ showed an absorption band at λ_{max} = ∼381 nm for nonaggregated MC chromophore (Figure 2a). In water, a significant hypsochromic shift was observed with an absorption maximum (H-band) at λ_{max} = ∼361 nm. Photoluminescence (PL) studies of **P2** showed AIEE properties in water (Figure 2b). Going from $CHCl_3$ to water, an enhancement in the Stokes shift from 5500 to 6100 cm^{-1} with

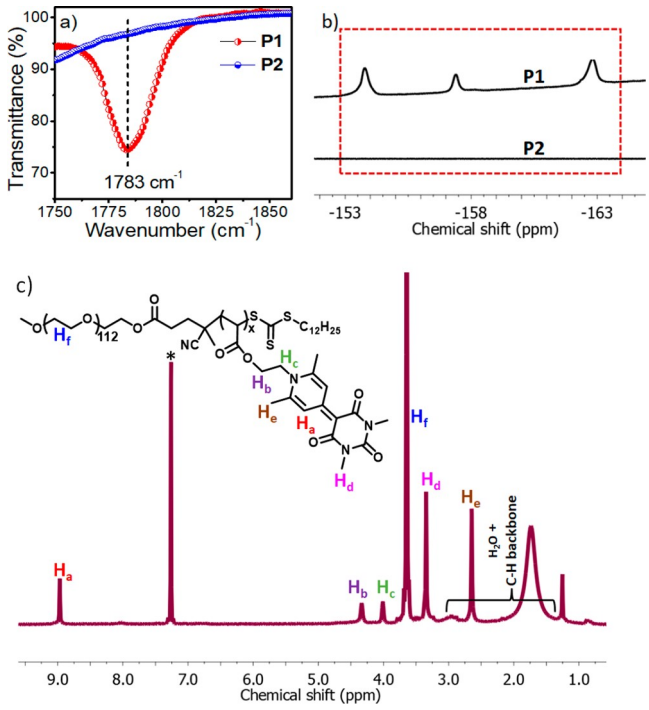

Figure 1. (a) FTIR spectra of **P1** and **P2** in the solid state and (b) their corresponding ^{19}F NMR spectra in $CDCl_3$ showing complete substitution of the activated PFP-ester group. (c) ^{1}H NMR spectrum of **P2** in $CDCl_3$. * denotes the residual solvent peak.

a concomitant increase in lifetime (τ) from 2.24 to 3.99 ns (Figure 2c) as determined from time-correlated single-photon counting (TCSPC) was noted.[29] Such spectral changes are typically known for the face-to-face H-type exciton coupling[19,27−29] of MCs due to their dipole−dipole interaction-mediated antiparallel dimerization in nonpolar solvents. Similar spectral trends in water suggest that MC-pendants were engaged in a similar kind of centrosymmetric antiparallel cofacial stacking. However, a remarkable peak shift of ∼20 nm in the UV−vis spectrum with a concomitant, ∼500 times enhancement in the emission intensity of **P2** in water is a rare phenomenon and reflects an unusual strong binding affinity of the attached MCs, which restricted their free movement in water and thereby prevented nonradiative transition. As a result, the quantum yield (ϕ) in the aggregated state in water reached up to 0.43%, compared to its almost nonemissive monomeric state in $CHCl_3$ (ϕ = 0.0006%; Supporting Information). The variable-temperature (VT) UV−vis spectra revealed no change in the aggregated spectra of **P2** with increasing temperature up to 85 °C (Figure 2a), suggesting an outstanding thermal stability of the cofacial MC-stacks in water. This is in sharp contrast to the earlier reports that showed a weak dimerization propensity of individual MCs in polar solvents owing to the interference from the solvent dipoles.[19,27]

Such an unparalleled finding in **P2** is attributed to its cooperative binding effect. Cooperative binding plays a vital role in many biological processes. Taking inspiration from nature, extensive effort has been devoted toward creating long-range ordered structures of diverse π-systems through cooperative supramolecular assemblies.[52] It is observed when multiple ligands on one species bind to multiple receptors of the same/another species having complementary binding

https://doi.org/10.1021/acspolymersau.1c00054
ACS Polym. Au 2022, 2, 223−231

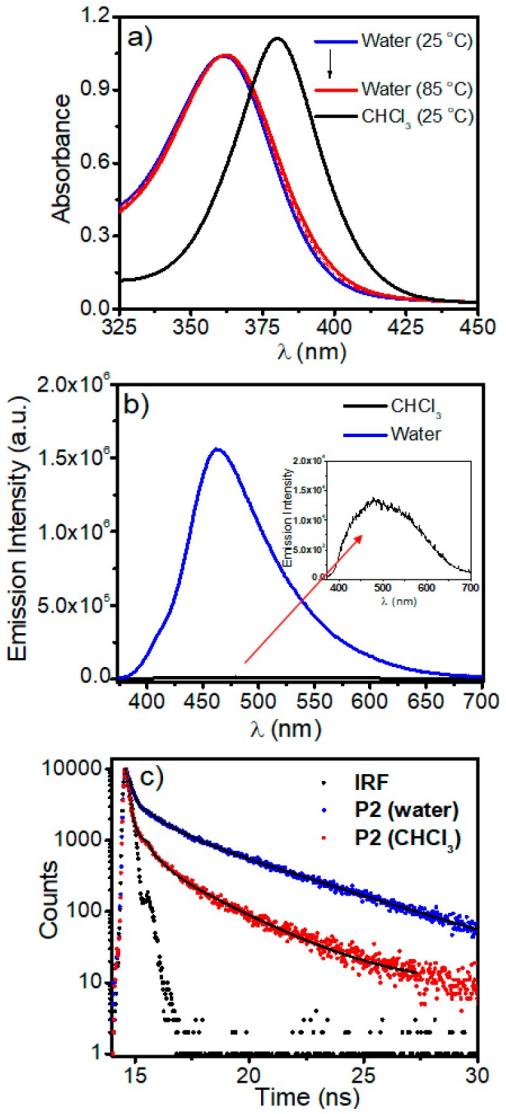

Figure 2. Solvent- and temperature-dependent (a) UV−vis spectra of **P2** and (b) its photoluminescence spectra (λ_{ex} = 360 nm) in $CHCl_3$ and water. (c) TCSPC fluorescence decay profiles of **P2** and fitted functions (solid black lines) in $CHCl_3$ (red) and water (blue). The instrument response function (IRF) is shown in black dots. Concentration = 0.125 mg/mL; λ_{ex} = 375 nm, λ_{em} = 469 nm.

motifs. Due to the cooperative effect between binding sites that are connected together, the first binding event strengthens the subsequent binding steps. As a consequence, a significant amplification in the overall binding strength compared to the summation of the corresponding monovalent single ligand/receptor binding is observed. Similarly, **P2** composed of several self-complementary MC-pendants in close proximity within π-stacking distances finds a way of amplifying a large number of weak dipole−dipole interactions through synchronized extended antiparallel stacking along the polymer backbone to strengthen its overall binding affinity by a cooperative effect.[30] As a result, exceptionally enhanced H-type exciton coupling with a remarkable AIEE feature was observed for the dipolar assembly of **P2** in water.

Next, we investigated the impact of such centrosymmetric antiparallel stacking of MCs on the morphology of **P2** in water. Does it lead to discrete dimers[19,28] or a higher-order structure of **P2**? Cryogenic transmission electron microscopy (cryo-TEM) showed irregularly shaped particles of **P2** in water (0.5 mg/mL; Figure 3a). The dynamic light scattering (DLS) data

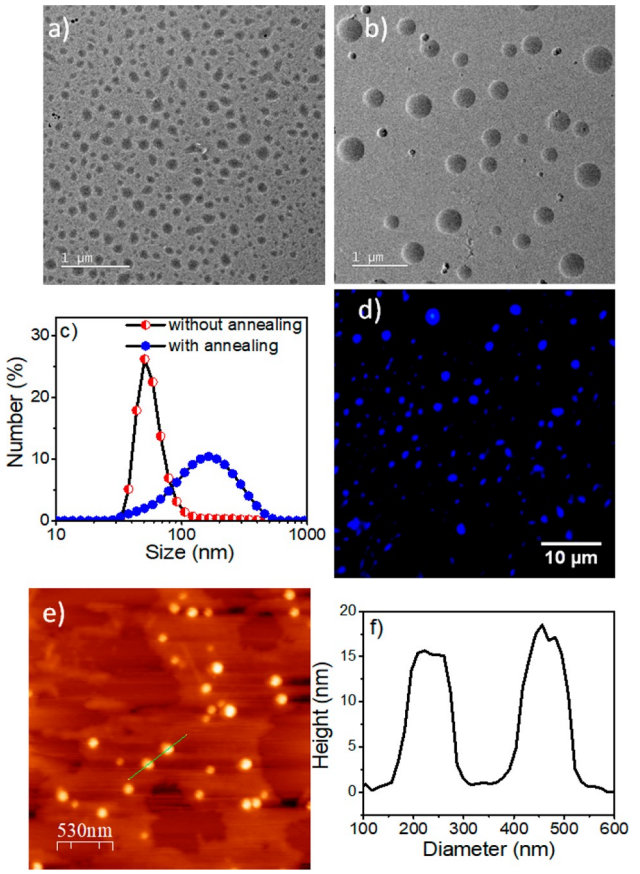

Figure 3. Cryo-TEM image of self-assembled **P2** in water (a) before and (b) after annealing. (c) Corresponding DLS data. (d) Blue emitting particles visualized under a fluorescence microscope. (e, f) AFM image and height profile from an annealed solution of **P2** in water. Concentration = 0.5 mg/mL.

revealed an average particle size of ∼50 nm (Figure 3c) which eliminates the possibility of the formation of discrete dimers at the tested concentration. Interestingly, the structural homogeneity and dimension of the particles could be significantly increased upon annealing the aqueous solution of **P2** at 50 °C for 3 h. An annealed solution produced distinct regularly shaped spherical nanoparticles (Figure 3b), which exhibit a blue emission under a fluorescence microscope (Figure 3d), in agreement with the PL data (Figure 2b). Further, DLS data recorded from the annealed solution (Figure 3c) revealed the formation of much larger aggregates with an average particle size in the range of ∼180 nm, corroborating the results obtained from cryo-TEM images.

Atomic force microscopy (AFM) revealed spherical objects with a much reduced average height of ∼18 nm compared to the average diameter of ∼200 nm, suggesting spherical disclike anisotropic structures (Figure 3e,f). Although thermal annealing enabled the formation of larger particles with more structural regularity, surprisingly, the cofacial MC-stacking was not affected by the annealing process, as no alteration in the aggregated absorption and emission spectra of **P2** was observed subsequent to the annealing process (Figure S3a,b).

Based on these experimental observations and previous reports on the stepwise packing of MC-based small

https://doi.org/10.1021/acspolymersau.1c00054
ACS Polym. Au 2022, 2, 223−231

molecules[29] and foldamers in organic solvents,[34,35] we propose a model for the self-assembly of **P2** in water. **P2** readily self-assembles in water through dipole−dipole interactions which initially leads to ill-defined particles (**Aggregate 1**). To completely cancel out its ground state dipole moment, the pendant MCs located in every repeat unit of **P2** were continuously aligned in an antiparallel orientation within the π-stacking distance with other **P2** chains along the entire MC-block which results in extended cofacial H-type stacking in **Aggregate 1** (Scheme 1) similar to previously reported bis(merocyanine)-based tweezer molecules.[30−33] However, in this case, the system gains enhanced stability possibly from the cooperative binding of the polymer chain. This is in sharp contrast to discrete MC-dimers reported earlier in individual merocyanines.[19,27,28] The planar aromatic framework obtained through such tightly bound centrosymmetric MC-stacking displays a structural resemblance with rigid π-conjugated amphiphilic polymers.[53,54] During the thermal annealing process, the relatively weaker dispersion forces between the water-incompatible rigid and planar π-surfaces allowed their reorganization into extended π-stacks, orthogonal to the direction of the dipolar interactions. As the solvent is water, unfavorable exposure of the terminal aromatic faces could be avoided through the formation of enclosed core−shell nanodisc-like structures (**Aggregate 2**). The required colloidal stability in water was acquired from the attached hydrophilic PEG chains. Due to the presence of such an extended rigid aromatic interior, a much greater radius of curvature for the **P2** nanodiscs (∼180 nm) was noted as compared to the previously reported polymeric micelles (∼33 nm)[37] from MC-labeled PEG-*b*-PS, which failed to produce such extended antiparallel MC-stacking owing to the disruption from the polystyrene segments.

The evidence of strong aromatic interactions within the nanodiscs could be obtained by comparing the ^{1}H NMR spectra (Figure 4a) in $CDCl_3$ and D_2O. The aromatic protons of MC (H_a) appeared at 8.08 ppm in D_2O, which is much more upfield shifted with respect to the chemical shift value in $CDCl_3$ (∼8.94 ppm). This suggests a shielding effect due to strong π-stacking interactions of MCs in water. With the temperature increasing from 30 to 80 °C, a partial downfield shift from 8.08 to 8.58 ppm was observed in D_2O, which was still significantly upfield shifted compared to $CDCl_3$ (Figure 4b). This suggests that the spectrum at 80 °C did not fully acquire the nonaggregated features as seen in $CDCl_3$. Likewise, VTDLS studies (concentration = 0.5 mg/mL) of the annealed sample revealed no change in the particle size up to 70 °C, suggesting an extremely high thermal stability of the nanodiscs in water (Figure 4c). When further heated to 80 °C, only a small drop of a particle size from ∼180 to ∼135 nm was noted. Together from the VTDLS and ^{1}H NMR studies it becomes evident that, at 80 °C, the aromatic framework was partially disturbed, which caused a shrinkage in the particle size but not complete disassembly. This is strikingly different from the results of the VT UV−vis spectral studies (Figure 2a) that showed no disruption of the dipolar stacking of MCs at all, at the same tested temperature window. Thus, this finding further supports the model for the stepwise hierarchical assembly of **P2** in water based on two types of stacking interactions of the side-chain MCs: (i) primarily dipole−dipole interaction-mediated extended antiparallel cofacial stacking of MCs along the polymer chain that generates thermally robust ill-defined particles (**Aggregate 1**) and (ii) extended aromatic

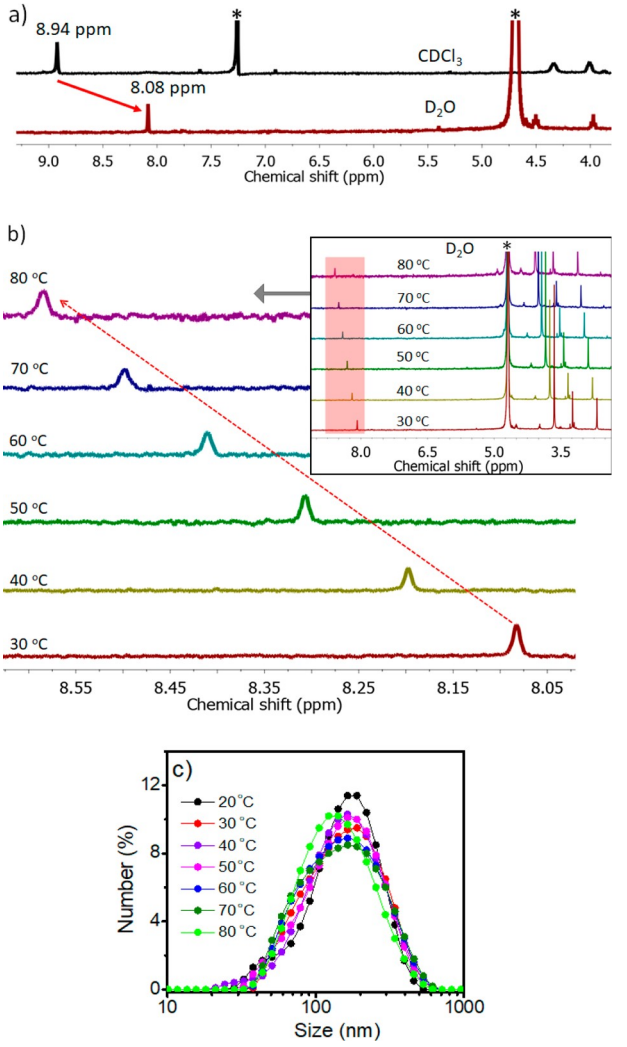

Figure 4. (a) Solvent-dependent ^{1}H NMR spectra of **P2**. (b) Variable-temperature ^{1}H NMR spectra of **P2** in D_2O from 30 to 80 °C. * denotes the solvent peak. (c) VT DLS data of **P2** (concentration = 0.5 mg/mL).

interactions in the orthogonal direction to dipolar stacking that leads to hierarchical structures with a nanodisc-like morphology (**Aggregate 2**), which could be partially destabilized by heating (Scheme 1).

Notably, the shielding effect observed in the aromatic proton signals of merocyanine has the contribution from both of these types of stacking interactions, while the blue-shift in the aggregated UV−vis spectra primarily indicates dipolar interaction-mediated antiparallel H-type stacking. This explains the disparity observed from the VT ^{1}H NMR and UV−vis studies. Thus, prior to the thermal treatment, **P2** readily formed collapsed aggregates in water. During the thermal annealing process, these ill-defined aggregates reorganized into uniform and bigger spherical discs by a readjustment of their aromatic surfaces without affecting the primary dipole−dipole interactions between the side-chain MCs, which was insensitive to the thermal change within the tested temperature window.

Guest Encapsulation Studies Using the FRET Technique

Next, the container property of the aromatic interior of **P2** was examined by hydrophobic dye encapsulation studies using two

https://doi.org/10.1021/acspolymersau.1c00054
ACS Polym. Au 2022, 2, 223−231

lipophilic dyes, 3,3′-dioctadecyloxacarbocyanine perchlorate (DiO) and 1,1′-dioctadecyl-3,3,3′,3′-tetramethylindocarbocyanine perchlorate (DiI), that are well-known Förster resonance energy transfer (FRET) dye pairs.[55] FRET is sensitive to the distance between the donor (DiO) and acceptor (DiI) dye pair. It is expected to occur in their coencapsulated state within the **P2** aggregates, when they are in close proximity within the range of a few nanometers. Upon exciting **P2** at the donor absorbance (λ_{ex} = 480 nm), a predominant emission from the acceptor (λ_{em} = 587 nm) dye was observed with a significant reduction in the donor emission (λ_{em} = 537 nm; Figure S4), indicating substantial energy transfer from DiO to DiI within the aromatic confined interior of the nanodiscs. In the absence of **P2**, a negligible emission with no energy transfer was noted in their free state in water at the same dye concentration (1×10^{-5} M; Figure S4).

Next, the kinetic stabilities of the **P2** nanocarriers were studied by the FRET technique. The donor and the acceptor dyes were separately sequestered within the aromatic core of the nanodiscs, and the evolution of the FRET emission was monitored as a function of time from their preformed 1:1 mixture in water. With the very onset of mixing, an intense band for the donor emission (537 nm) with a weak shoulder peak for the acceptor (587 nm) was observed, suggesting negligible FRET. Time-dependent emission spectra showed no change over a period of 2 days, indicating a remarkable kinetic stability of these nanocarriers (Figure S5). Usually, polymeric micelles derived from conventional amphiphilic block copolymers exhibit very fast exchange dynamics with their corresponding unimers, and the FRET equilibria are mostly reached within a few hours.[55,56] The unusually high kinetic stability of the **P2** nanodiscs was ascribed to its rigid aromatic interior, unlike conventional polymeric micelle cores derived from flexible hydrocarbon chains. We envisaged that the stiff aromatic framework of these nanoparticles can be denatured in the presence of a water-miscible "good" solvent like THF, which can disrupt the primary antiparallel MC-stacking. Thus, the disassembly of **P2** was monitored by evaluating the FRET ratio $[I_A/(I_A + I_D)]$ between the coencapsulated dye pair by stepwise addition of THF, where I_A and I_D represent the acceptor (587 nm) and donor (537 nm) emission, respectively. A plot of the normalized emission with varying fractions of THF in water (v/v) revealed the gradual disappearance of the DiI emission with a concomitant appearance of the DiO emission (λ_{ex} = 480 nm; Figure 5a). The FRET ratio vs THF addition plot (Figure 5b) reveals saturation at ∼30% THF (v/v), which suggests a release of the coencapsulated dyes due to the disassembly of the nanodiscs. Indeed, in the presence of 35% THF (v/v), a complete loss of the structural integrity of the spherical particles was evident from the TEM studies (Figure S6).

The dipolar interaction-mediated rigid aromatic stacking in **P2** was expected to enhance its self-assembly propensity in water. To study that, the critical aggregation concentration (CAC) was determined following the same FRET technique. It was anticipated that, below a threshold concentration, the disassembly of the nanodiscs would lead to the disappearance of FRET owing to the release of the two dyes from the particle core. An enhancement in the FRET ratio was observed with increasing **P2** concentration up to a threshold value, above which it remains invariant (Figure S7a). From the intersection of the two straight lines, the CAC was determined to be 0.023 mg/mL (≈ 3×10^{-6} M; Figure S7b). This data exactly

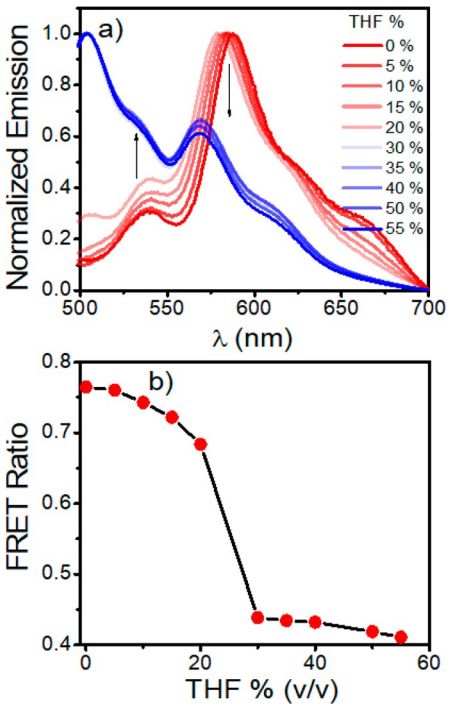

Figure 5. (a) Change in the normalized emission spectra of DiO+DiI coencapsulated **P2** nanodiscs in water as a function of THF addition. (b) Plot of the FRET ratio with THF fraction. λ_{ex} = 480 nm; concentration of **P2** = 0.125 mg/mL, DiO = DiI = 1×10^{-5} M.

matched with the CAC value (0.023 mg/mL ≈ 2.5×10^{-6} M) obtained from the UV−vis dilution studies of **P2** in water (Figure 6 a,b). Intriguingly, the UV−vis spectrum of **P2** recorded at the lowest tested concentration of 0.0005 mg/mL ≈ 5.5×10^{-8} M retained the features of the antiparallel cofacial stacking of MCs (Figure 6c). It can be fairly presumed that, with dilution, the aromatic stacking was partly destabilized, while the primary dipole−dipole interaction-driven cofacial MC-stacking was preserved, even at a concentration much

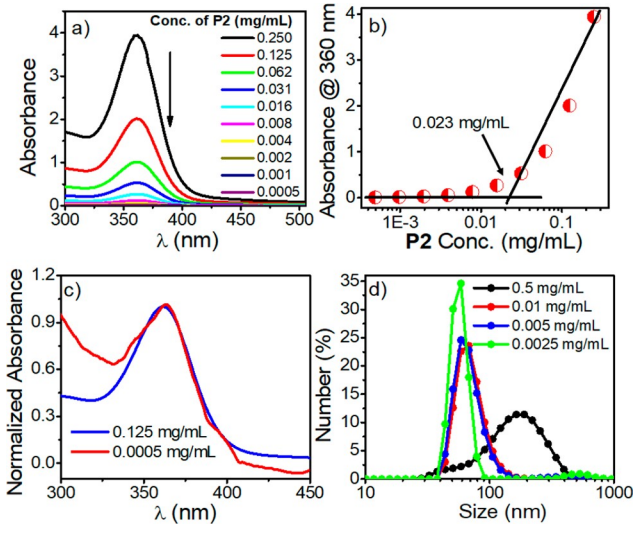

Figure 6. (a) Concentration-dependent absorption spectra of **P2** in water. (b) Determination of the critical aggregation concentration (CAC) from the absorbance plot. Path length = 5 nm. (c) Normalized absorbance plot of **P2** at two different concentrations. (d) Concentration-dependent DLS data of **P2** in water.

https://doi.org/10.1021/acspolymersau.1c00054
ACS Polym. Au 2022, 2, 223−231

below the CAC. This is further supported by the concentration-variable DLS data (Figure 6d) that showed a significant reduction in the particle size (from ∼180 to ∼55 nm) with dilution. The loss of structural homogeneity and the formation of ill-defined aggregates of variable sizes due to a different extent of aromatic interactions were confirmed from the AFM studies at a much lower **P2** concentration (0.005 mg/mL; Figure S8). The above results corroborate with the temperature-dependent studies and further validate the proposed model of stepwise assembly of **P2** in water through a dual effect of dipolar and aromatic interactions of the pendant MCs.

CONCLUSION

This Article describes the underexploited directional dipole−dipole interaction-mediated self-assembly of a highly water-soluble MC-appended block copolymer into well-defined spherical nanodiscs that showed outstanding AIEE properties, remarkable stability, very low CAC, and hydrophobic guest loading abilities in water. D-π-A type MCs have the unique ability to align their molecular dipoles in an opposite orientation through strong electrostatic interactions and yield discrete dimers.[19] Hierarchical assemblies in individual MCs are rarely reported, also confined to extremely nonpolar solvents like methylcyclohexane.[31,34,35] Herein, we described the continuous antiparallel cofacial stacking of pendant MCs through the formation of a rigid cofacially stacked H-aggregate, which displayed unprecedented stability in water due to the cooperative effect of the polymer chain. The spontaneous formation of a higher-order structure was driven by extended orthogonal π-stacking between the MC-stacked aromatic frameworks in water. Our results reveal that a tightly bound centrosymmetric packing of MCs is not limited to low-polarity environments but can be adopted as a powerful structural motif for precision macromolecular assembly, even in a highly polar solvent like water. For its exciting AIEE properties, high directionality, and tunable binding strength, the dipolar stacking of MC appears to be an attractive alternative to commonly exploited H-bonding for engineering macromolecular assemblies. Furthermore, the present results highlight a wider tolerance level of dipolar interactions toward solvent polarity as it does not necessitate supplementary hydrophobic assistance to operate in an aqueous medium, unlike H-bonding. The described modular strategy can be easily extended to a wide variety of functional polymeric scaffolds using structurally different MC-dyes. This work opens up exciting possibilities for a future engineering of macromolecular assembly/folding with an added advantage of assembly encoded emission properties in MC-functionalized polymers.

ASSOCIATED CONTENT

Supporting Information

The Supporting Information is available free of charge at https://pubs.acs.org/doi/10.1021/acspolymersau.1c00054.

Synthesis of the polymers, characterization data, additional spectroscopic data, and microscopic images (PDF)

AUTHOR INFORMATION

Corresponding Author

Anindita Das − *School of Applied and Interdisciplinary Sciences, Indian Association for the Cultivation of Science, Kolkata 700032, India;* orcid.org/0000-0001-8723-6291; Email: psuad2@iacs.res.in

Author

Aritra Rajak − *School of Applied and Interdisciplinary Sciences, Indian Association for the Cultivation of Science, Kolkata 700032, India*

Complete contact information is available at: https://pubs.acs.org/10.1021/acspolymersau.1c00054

Notes

The authors declare no competing financial interest.

ACKNOWLEDGMENTS

A.R. thanks CSIR, India, for a fellowship, and A.D. thanks CSIR, India [Project 02(0360)/19/EMR-II], for funding. The authors thank Dr. Anurag Mukherjee (IACS) and Ms. Payel Khanra (from the group) for assistance with the fluorescence microscopy and AFM measurements, respectively.

REFERENCES

(1) Wang, J.; Liu, K.; Ruirui, X.; Yan, X. Peptide self-assembly: thermodynamics and kinetics. *Chem. Soc. Rev.* **2016**, *45*, 5589−5604.
(2) Higashi, S. L.; Rozi, N.; Hanifah, S. A.; Ikeda, M. Supramolecular Architectures of Nucleic Acid/Peptide Hybrids. *Int. J. Mol. Sci.* **2020**, *21*, 9458−9482.
(3) Sikder, A.; Chakraborty, S.; Rajdev, P.; Dey, P.; Ghosh, S. Molecular Recognition Driven Bioinspired Directional Supramolecular Assembly of Amphiphilic (Macro)molecules and Proteins. *Acc. Chem. Res.* **2021**, *54*, 2670−2682.
(4) Hendricks, M. P.; Sato, K.; Palmer, L. C.; Stupp, S. I. Supramolecular Assembly of Peptide Amphiphiles. *Acc. Chem. Res.* **2017**, *50*, 2440−2448.
(5) Albert, S. K.; Golla, M.; Krishnan, N.; Perumal, D.; Varghese, R. DNA−π Amphiphiles: A Unique Building Block for the Crafting of DNA-Decorated Unilamellar Nanostructures. *Acc. Chem. Res.* **2020**, *53*, 2668−2679.
(6) Chang, Y.; Jiao, Y.; Symons, H. E.; Xu, J.-F.; Faul, C. F. J.; Zhang, X. Molecular engineering of polymeric supra-amphiphiles. *Chem. Soc. Rev.* **2019**, *48*, 989−1003.
(7) Sikder, A.; Ghosh, S. Hydrogen-bonding regulated assembly of molecular and macromolecular amphiphiles. *Mater. Chem. Front.* **2019**, *3*, 2602−2616.
(8) Yagai, S. Supramolecularly Engineered Functional π-Assemblies Based on Complementary Hydrogen-Bonding Interactions. *Bull. Chem. Soc. Jpn.* **2015**, *88*, 28−58.
(9) Whittell, G. R.; Hager, M. D.; Schubert, U. S.; Manners, I. Functional soft materials from metallopolymers and metallosupramolecular polymers. *Nat. Mater.* **2011**, *10*, 176−188.
(10) Wang, Y.; Astruc, D.; Abd-El-Aziz, A. S. Metallopolymers for advanced sustainable applications. *Chem. Soc. Rev.* **2019**, *48*, 558−636.
(11) Das, A.; Ghosh, S. Supramolecular Assemblies by Charge-Transfer Interactions between Donor and Acceptor Chromophores. *Angew. Chem., Int. Ed.* **2014**, *53*, 2038−2054.
(12) Xia, D.; Wang, P.; Ji, X.; Khashab, N. M.; Sessler, J. L.; Huang, F. Functional Supramolecular Polymeric Networks: The Marriage of Covalent Polymers and Macrocycle-Based Host-Guest Interactions. *Chem. Rev.* **2020**, *120*, 6070−6123.
(13) Oz, Y.; Abdouni, Y.; Yilmaz, G.; Becer, C. R.; Sanyal, A. Magnetic glyconanoparticles for selective lectin separation and purification. *Polym. Chem.* **2019**, *10*, 3351−3361.

(14) Arslan, M.; Sanyal, R.; Sanyal, A. Cyclodextrin embedded covalently crosslinked networks: synthesis and applications of hydrogels with nano-containers. *Polym. Chem.* **2020**, *11*, 615−629.
(15) Berger, G.; Soubhyea, J.; Meyer, F. Halogen bonding in polymer science: from crystal engineering to functional supramolecular polymers and materials. *Polym. Chem.* **2015**, *6*, 3559−3580.
(16) Biswas, S.; Das, A. Recent Developments in Polymeric Assemblies and Functional Materials by Halogen Bonding. *ChemNanoMat* **2021**, *7*, 748−772.
(17) Kampes, R.; Zechel, S.; Hager, M. D.; Schubert, U. S. Halogen bonding in polymer science: towards new smart materials. *Chem. Sci.* **2021**, *12*, 9275−9286.
(18) Jamadar, A.; Das, A. A pH-responsive graftable supramolecular polymer with tailorable surface functionality by orthogonal halogen bonding and hydrogen bonding. *Polym. Chem.* **2020**, *11*, 385−392.
(19) Würthner, F. Dipole-Dipole Interaction Driven Self-Assembly of Merocyanine Dyes: From Dimers to Nanoscale Objects and Supramolecular Materials. *Acc. Chem. Res.* **2016**, *49*, 868−876.
(20) Yagai, S.; Okamura, S.; Nakano, Y.; Yamauchi, M.; Kishikawa, K.; Karatsu, T.; Kitamura, A.; Ueno, A.; Kuzuhara, D.; Yamada, H.; Seki, T.; Ito, H. Design amphiphilic dipolar π-systems for stimuli-responsive luminescent materials using metastable states. *Nat. Commun.* **2014**, *5*, 4013.
(21) Kulkarni, C.; Bejagam, K. K.; Senanayak, S. P.; Narayan, K. S.; Balasubramanian, S.; George, S. J. Dipole-Moment-Driven Cooperative Supramolecular Polymerization. *J. Am. Chem. Soc.* **2015**, *137* (11), 3924−3932.
(22) Das, A.; Maity, B.; Koley, D.; Ghosh, S. Slothful gelation of a dipolar building block by "top-down" morphology transition from microparticles to nanofibers. *Chem. Commun.* **2013**, *49*, 5757−5759.
(23) Dong, M.; Miao, K.; Hu, Y.; Wu, J.; Li, J.; Pang, P.; Miao, X.; Deng, W. Cooperating dipole-dipole and van der Waals interactions driven 2D self-assembly of fluorenone derivatives: ester chain length effect. *Phys. Chem. Chem. Phys.* **2017**, *19*, 31113−31120.
(24) Berrocal, J. A.; Mabesoone, M. F. J.; Iglesias, M. G.; Huizinga, A.; Meijer, E. W.; Palmans, A. R. A. Selenoamides modulate dipole−dipole interactions in hydrogen bonded supramolecular polymers of 1,3,5-substituted benzenes. *Chem. Commun.* **2019**, *55*, 14906−14909.
(25) Jamadar, A.; Karan, C. K.; Roy, L.; Das, A. Structurally Tunable pH-Responsive Luminescent Assemblies from Halogen Bonded Supra-π-amphiphiles. *Langmuir* **2020**, *36*, 3089−3095.
(26) Jamadar, A.; Singh, A. K.; Roy, L.; Das, A. Stimuli-Responsive Luminescent Supramolecular Assemblies and Co-assemblies by Orthogonal Dipole-Dipole Interaction and Halogen Bonding. *J. Mater. Chem. C* **2021**, *9*, 11893−11904.
(27) Yao, S.; Würthner, F. Dipolar Dye Aggregates: A problem for Nonlinear Optics, but a Chance for Supramolecular Chemistry. *Angew. Chem., Int. Ed.* **2000**, *39*, 1978−1981.
(28) Rösch, U.; Yao, S.; Wortmann, R.; Würthner, F. Fluorescent H-Aggregates of Merocyanine Dyes. *Angew. Chem., Int. Ed.* **2006**, *45*, 7026−7030.
(29) Vonhausen, Y.; Lohr, A.; Stolte, M.; Würthner, F. Two-step anti-cooperative self-assembly process into defined π-stacked dye oligomers: insights into aggregation-induced enhanced emission. *Chem. Sci.* **2021**, *12*, 12302−12314.
(30) Fernández, G.; Stolte, M.; Stepanenko, V.; Würthner, F. Cooperative Supramolecular Polymerization: Comparison of Different Models Applied on the Self-Assembly of Bis(merocyanine) Dyes. *Chem. Eur. J.* **2013**, *19*, 206−217.
(31) Kirchner, E.; Bialas, D.; Fennel, F.; Grüne, M.; Würthner, F. Defined Merocyanine Dye Stacks from a Dimer up to an Octamer by Spacer-Encoded Self-Assembly Approach. *J. Am. Chem. Soc.* **2019**, *141*, 7428−7438.
(32) Zitzler-Kunkel, A.; Kirchner, E.; Bialas, D.; Simon, C.; Würthner, F. Spacer-Modulated Differentiation Between Self-Assembly and Folding Pathways for Bichromophoric Merocyanine Dyes. *Chem. Eur. J.* **2015**, *21*, 14851−14861.
(33) Lohr, A.; Grüne, M.; Würthner, F. Self-Assembly of Bis(merocyanine) Tweezers into Discrete Bimolecular π-Stacks. *Chem. Eur. J.* **2009**, *15*, 3691−3705.
(34) Hu, X.; Lindner, J. O.; Würthner, F. Stepwise Folding and Self-Assembly of a Merocyanine Folda-Pentamer. *J. Am. Chem. Soc.* **2020**, *142*, 3321−3325.
(35) Hu, X.; Schulz, A.; Lindner, J. O.; Grüne, M.; Bialas, D.; Würthner, F. Folding and fluorescence enhancement with strong odd−even effect for a series of merocyanine dye oligomers. *Chem. Sci.* **2021**, *12*, 8342−8352.
(36) Das, A.; Lin, S.; Theato, P. Supramolecularly Cross-Linked Nanogel by Merocyanine Pendent Copolymer. *ACS Macro Lett.* **2017**, *6*, 50−55.
(37) Rajak, A.; Karan, C. K.; Theato, P.; Das, A. Supramolecularly cross-linked amphiphilic block copolymer assembly by the dipolar interaction of a merocyanine dye. *Polym. Chem.* **2020**, *11*, 695−703.
(38) Xiong, Y.; Tang, H.; Zhang, J.; Wang, Z. Y.; Campo, J.; Wenseleers, W.; Goovaerts, E. Functionalized Picolinium Quinodimethane Chromophores for Electro-Optics: Synthesis, Aggregation Behavior, and Nonlinear Optical Properties. *Chem. Mater.* **2008**, *20*, 7465−7473.
(39) Li, M.; Li, Y.; Zhang, H.; Wang, S.; Ao, Y.; Cui, Z. Molecular engineering of organic chromophores and polymers for enhanced bulk second-order optical nonlinearity. *J. Mater. Chem. C* **2017**, *5*, 4111−4122.
(40) Zhang, D.; Shah, P. K.; Culver, H. R.; David, S. N.; Stansbury, J. W.; Yin, X.; Bowman, C. N. Photo-responsive liposomes composed of spiropyran-containing triazole-phosphatidylcholine: investigation of merocyanine-stacking effects on liposome-fiber assembly-transition. *Soft Matter* **2019**, *15*, 3740−3750.
(41) Sommer, M. Substituent Effects Control Spiropyran-Merocyanine Equilibria and Mechanochromic Utility. *Macromol. Rapid Commun.* **2021**, *42*, 2000597.
(42) Dübner, M.; Cadarso, V. J.; Gevrek, T. N.; Sanyal, A.; Spencer, N. D.; Padeste, C. Reversible Light-Switching of Enzymatic Activity on Orthogonally Functionalized Polymer Brushes. *ACS Appl. Mater. Interfaces* **2017**, *9*, 9245−9249.
(43) Wagner, K.; Zanoni, M.; Elliott, A. B. S.; Wagner, P.; Byrne, R.; Florea, L. E.; Diamond, D.; Gordon, K. C.; Wallace, G. G.; Officer, D. L. A merocyanine-based conductive polymer. *J. Mater. Chem. C* **2013**, *1*, 3913−3916.
(44) Zitzler-Kunkel, A.; Lenze, M. R.; Kronenberg, N. M.; Krause, A.-M.; Stolte, M.; Meerholz, K.; Würthner, F. NIR-Absorbing Merocyanine Dyes for BHJ Solar Cells. *Chem. Mater.* **2014**, *26*, 4856−4866.
(45) Mayoral Muñoz, M. J.; Fernández, G. Metallosupramolecular amphiphilic π-systems. *Chem. Sci.* **2012**, *3*, 1395−1398.
(46) Molla, M. R.; Ghosh, S. Aqueous self-assembly of chromophore-conjugated amphiphiles. *Phys. Chem. Chem. Phys.* **2014**, *16*, 26672−26683.
(47) Das, A.; Theato, P. Activated Ester Containing Polymers: Opportunities and Challenges for the Design of Functional Macromolecules. *Chem. Rev.* **2016**, *116*, 1434−1495.
(48) Das, A.; Theato, P. Multifaceted Synthetic Route to Functional Polyacrylates by Transesterification of Poly(pentafluorophenyl acrylates). *Macromolecules* **2015**, *48*, 8695−8707.
(49) Saha, B.; Ruidas, B.; Mete, S.; Mukhopadhyay, C. D.; Bauri, K.; De, P. AIE-active non-conjugated poly(N-vinylcaprolactam) as a fluorescent thermometer for intracellular temperature imaging. *Chem. Sci.* **2020**, *11*, 141−147.
(50) Bauri, K.; Saha, B.; Banerjee, A.; De, P. Recent advances in the development and applications of nonconventional luminescent polymers. *Polym. Chem.* **2020**, *11*, 7293−7315.
(51) Qin, A.; Lam, J. W. Y.; Tang, B. Z. Luminogenic polymers with aggregation-induced emission characteristics. *Prog. Polym. Sci.* **2012**, *37*, 182−209.
(52) Rest, C.; Kandanellia, R.; Fernández, G. Strategies to create hierarchical self-assembled structures via cooperative non-covalent interactions. *Chem. Soc. Rev.* **2015**, *44*, 2543−2572.

https://doi.org/10.1021/acspolymersau.1c00054
ACS Polym. Au 2022, 2, 223−231

(53) Narasimha, K.; Jayakannan, M. Color-Tunable Amphiphilic Segmented π-Conjugated Polymer Nano-Assemblies and Their Bioimaging in Cancer Cells. *Macromolecules* **2016**, *49*, 4102−4114.
(54) MacFarlane, L. R.; Shaikh, H.; Garcia-Hernandez, J. D.; Vespa, M.; Fukui, T.; Manners, I. Functional nanoparticles through π-conjugated polymer self-assembly. *Nat. Rev. Mater.* **2021**, *6*, 7−26.
(55) Jiwpanich, S.; Ryu, J.-H.; Bickerton, S.; Thayumanavan, S. Noncovalent Encapsulation Stabilities in Supramolecular Nanoassemblies. *J. Am. Chem. Soc.* **2010**, *132*, 10683−10685.
(56) Rajdev, P.; Basak, D.; Ghosh, S. Insights into Noncovalently Core Cross-Linked Block Copolymer Micelles by Fluorescence Resonance Energy Transfer (FRET) Studies. *Macromolecules* **2015**, *48*, 3360−3367.

https://doi.org/10.1021/acspolymersau.1c00054
ACS Polym. Au 2022, 2, 223−231